10-2018

Lithium and Gallium Vacancies in $LiGaO_2$ Crystals

Christopher A. Lenyk

Maurio S. Holston

Brant E. Kananen
Air Force Institute of Technology

Larry E. Halliburton
West Virginia University

Nancy C. Giles
Air Force Institute of Technology

Recommended Citation

Lenyk, C. A., Holston, M. S., Kananen, B. E., Halliburton, L. E., & Giles, N. C. (2018). Lithium and gallium vacancies in LiGaO 2 crystals. Journal of Applied Physics, 124(13), 135702. https://doi.org/10.1063/1.5050532

Lithium and gallium vacancies in $LiGaO_2$ crystals

C. A. Lenyk,[1] M. S. Holston,[1] B. E. Kananen,[1] L. E. Halliburton,[2] and N. C. Giles[1,a)]
[1]*Department of Engineering Physics, Air Force Institute of Technology, Wright-Patterson Air Force Base, Ohio 45433, USA*
[2]*Department of Physics and Astronomy, West Virginia University, Morgantown, West Virginia 26506, USA*

(Received 31 July 2018; accepted 13 September 2018; published online 5 October 2018)

Lithium gallate ($LiGaO_2$) is a wide-band-gap semiconductor with an optical gap greater than 5.3 eV. When alloyed with ZnO, this material offers broad functionality for optical devices that generate, detect, and process light across much of the ultraviolet spectral region. In the present paper, electron paramagnetic resonance (EPR) is used to identify and characterize neutral lithium vacancies (V_{Li}^0) and doubly ionized gallium vacancies (V_{Ga}^{2-}) in $LiGaO_2$ crystals. These S = 1/2 native defects are examples of acceptor-bound small polarons, where the unpaired spin (i.e., the hole) is localized on one oxygen ion adjacent to the vacancy. Singly ionized lithium vacancies (V_{Li}^-) are present in as-grown crystals and are converted to their paramagnetic state by above-band-gap photons (x rays are used in this study). Because there are very few gallium vacancies in as-grown crystals, a post-growth irradiation with high-energy electrons is used to produce the doubly ionized gallium vacancies (V_{Ga}^{2-}). The EPR spectra allow us to establish detailed models for the two paramagnetic vacancies. Anisotropy in their *g* matrices is used to identify which of the oxygen ions adjacent to the vacancy has trapped the hole. Both spectra also have resolved structure due to hyperfine interactions with ^{69}Ga and ^{71}Ga nuclei. The V_{Li}^0 acceptor has nearly equal interactions with Ga nuclei at two Ga sites adjacent to the trapped hole, whereas the V_{Ga}^{2-} acceptor has an interaction with Ga nuclei at only one adjacent Ga site. *Published by AIP Publishing.* https://doi.org/10.1063/1.5050532

I. INTRODUCTION

Lithium gallate ($LiGaO_2$) is an ultrawide-band-gap semiconductor[1,2] with a wurtzite-like crystal structure. Its optical absorption edge is in the 5.3–5.7 eV range.[3–7] This material is a ternary analog of ZnO. Replacing half the Zn^{2+} ions with Li^+ ions and half with Ga^{3+} ions in an ordered arrangement gives $LiGaO_2$. Alloying $LiGaO_2$ with ZnO is expected to produce crystals appropriate for ultraviolet optical applications.[8–10] As suitable shallow donors and acceptors are identified,[11] the $LiGaO_2$-ZnO mixed materials system will allow laser diodes and photodetectors to be fabricated that operate across much of the ultraviolet region. $LiGaO_2$ is also a candidate for phosphor and radiation-detector applications.[12–16] This ternary material has both monovalent (Li^+) and trivalent (Ga^{3+}) cation sites and thus provides a variety of doping possibilities. These include transition-metal ions and rare-earth ions, Group I and Group III isovalent impurities, and Group II and Group IV donors and acceptors. These many doping choices offer broad functionality for diverse applications of $LiGaO_2$ and its alloys with ZnO.

In the present paper, we use electron paramagnetic resonance (EPR) to investigate native acceptors in $LiGaO_2$ crystals. Similar studies have been reported for $LiAlO_2$ crystals.[17,18] Spectra from lithium vacancies and gallium vacancies are observed in our $LiGaO_2$ crystals. In both cases, the hole is localized on one oxygen ion adjacent to the vacancy, in a small-polaron configuration.[19,20] Anisotropy in the *g* matrices allows us to determine which oxygen ion traps the hole. The V_{Li}^0 and V_{Ga}^{2-} spectra in $LiGaO_2$ have resolved hyperfine structure due to interactions of the trapped hole with the adjacent ^{69}Ga and ^{71}Ga nuclei. Nearly equal interactions with nuclei at two gallium sites are seen in the V_{Li}^0 spectrum, whereas interactions with nuclei at only one gallium site are observed in the V_{Ga}^{2-} spectrum. These different hyperfine patterns easily allow the V_{Li}^0 and V_{Ga}^{2-} spectra to be individually recognized. Although their spectra are obtained at low temperature, the paramagnetic charge states of both vacancies are stable at room temperature. Information about the small-polaron characteristics and the thermal stabilities of these native defects will be useful when searching for acceptor dopants for $LiGaO_2$. Lithium diffusion studies will also benefit from a spectroscopic method that monitors the presence of lithium vacancies.[21,22]

II. EXPERIMENTAL

Undoped $LiGaO_2$ crystals, grown by the Czochralski method, were obtained from the MTI Corporation (Richmond, CA). They are highly resistive, thus indicating that the Fermi level is near mid-gap. Lithium vacancies are present in some, but not all, of the as-grown $LiGaO_2$ crystals supplied by MTI, whereas gallium vacancies are not present in any of the as-grown crystals. Spectra from two $LiGaO_2$ crystals, labeled Sample A and Sample B, are reported in the present investigation. Sample A was used to investigate neutral lithium vacancies and was only irradiated with x rays (i.e., ionizing radiation). By trapping a hole on an adjacent oxygen ion, the irradiation with x rays (60 kV, 30 mA) at room temperature converted nonparamagnetic lithium vacancies in this sample to a paramagnetic charge state that could

a)Author to whom correspondence should be addressed: Nancy.Giles@afit.edu

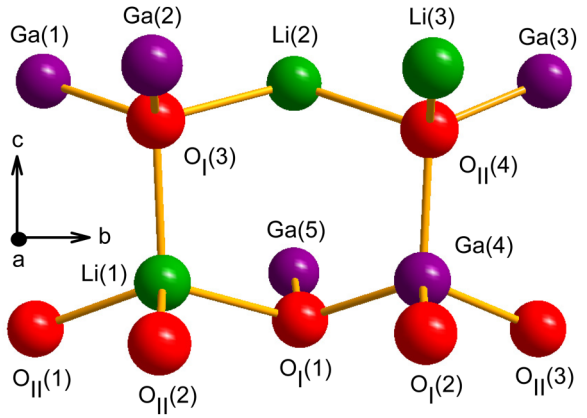

FIG. 1. Schematic representation of the $LiGaO_2$ crystal structure. Lithium ions are green, gallium ions are purple, and oxygen ions are red. The two inequivalent oxygen sites are labeled O_I and O_{II}. Each lithium and gallium ion has four oxygen neighbors and each oxygen ion has two lithium and two gallium neighbors.

be observed at low temperature with EPR. Sample B was only electron irradiated and was used to investigate doubly ionized gallium vacancies. This crystal was irradiated near room temperature with high-energy electrons (1 MeV, 5 μA) from a Van de Graff accelerator at Wright State University. During the irradiation, the crystal was in contact with a water-cooled heat sink to minimize heating by the electron beam. Momentum-conserving displacement events, initiated by the high-energy electrons, produced a large concentration of paramagnetic gallium vacancies in the $LiGaO_2$ crystal, without requiring a subsequent irradiation with x rays. The EPR spectra reported in this paper represent approximate defect concentrations of 2.3×10^{18} cm^{-3} for the V^0_{Li} acceptors and 1.8×10^{17} cm^{-3} for the V^{2-}_{Ga} acceptors.

$LiGaO_2$ crystals are orthorhombic (space group $Pna2_1$), with lattice constants $a = 5.402$ Å, $b = 6.372$ Å, and $c = 5.007$ Å at room temperature.[23] Figure 1 is a ball-and-stick representation of the crystal. The relative x,y,z positions of the ions in Fig. 1 are given in Table I. In this material, each oxygen ion has two lithium neighbors and two gallium neighbors, each lithium ion has four oxygen neighbors, and each gallium ion has four oxygen neighbors. The Li^+ sites are all equivalent, and the Ga^{3+} sites are all equivalent. Oxygen ions occupy two crystallographically inequivalent sites (these are labeled O_I and O_{II} in Fig. 1). The two oxygen sites are most easily distinguished by which cation, a Li^+ or a Ga^{3+}, is the nearest neighbor along the c axis (i.e., the [001] direction). The O_I ions have an adjacent lithium ion in the c direction and the O_{II} ions have an adjacent gallium ion in the c direction.

TABLE I. Relative positions (in Å units) of ions in $LiGaO_2$, based on the room-temperature lattice parameters reported by Marezio.[23] The ion labeling scheme in Fig. 1 is used.

Ion	x	y	z
Li(1)	3.1294	5.5647	4.9750
Li(2)	2.2726	7.1793	7.4785
Li(3)	4.9736	8.7507	7.4785
Ga(1)	2.2575	3.9908	7.5105
Ga(2)	4.9585	5.5672	7.5105
Ga(3)	2.2575	10.3628	7.5105
Ga(4)	3.1445	8.7532	5.0070
Ga(5)	0.4435	7.1768	5.0070
Ga(6)	5.8455	7.1768	5.0070
Ga(7)	4.9585	5.5672	2.5035
$O_I(1)$	2.1965	7.2564	4.4697
$O_I(2)$	4.8975	8.6736	4.4697
$O_I(3)$	3.2055	5.4876	6.9732
$O_{II}(1)$	2.3245	3.9003	4.3601
$O_{II}(2)$	5.0255	5.6577	4.3601
$O_{II}(3)$	2.3245	10.2723	4.3601
$O_{II}(4)$	3.0775	8.8437	6.8636

The EPR spectra were taken with a Bruker EMX spectrometer operating near 9.40 GHz. A Bruker NMR teslameter was used to measure the static magnetic field, and an Oxford helium-gas flow system controlled the sample temperature. The isotropic Cr^{3+} signal ($g = 1.9800$) in an MgO crystal was used to make corrections for the small differences in magnetic field at the NMR probe tip and the sample position.

III. NEUTRAL LITHIUM VACANCY (V^0_{Li})

Figure 2(a) shows the EPR spectrum from the neutral lithium vacancy (V^0_{Li}) in Sample A. This spectrum, taken at 55 K with the magnetic field along the c axis, was obtained after the as-received crystal was irradiated at room temperature with x rays. Singly ionized lithium vacancies (V^-_{Li}) in the as-grown crystal are converted to their paramagnetic neutral charge state (V^0_{Li}) during the irradiation. Many of the free electrons and holes created by the x rays quickly recombine. A small portion of the holes, however, are trapped on oxygen ions adjacent to lithium vacancies, thus forming the V^0_{Li} centers. A corresponding number of electrons are trapped at unidentified defects (possibly oxygen vacancies or impurities). Heating the crystal above 150 °C destroys the V^0_{Li} spectrum and returns the crystal to its pre-irradiated state.

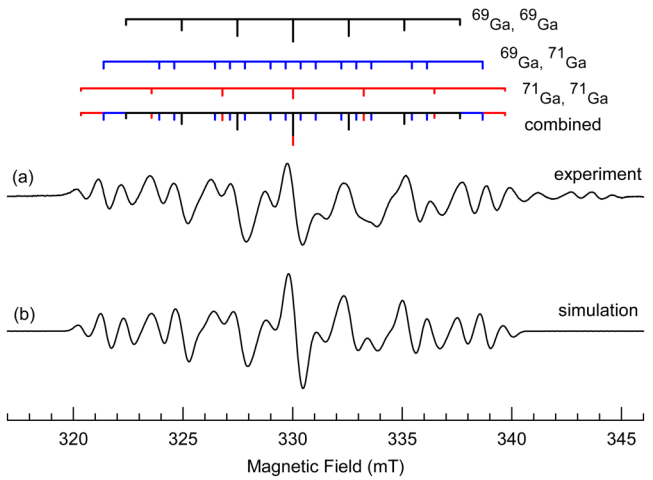

FIG. 2. (a) EPR spectrum of the neutral lithium vacancy (V^0_{Li}) in $LiGaO_2$ (Sample A). The crystal was irradiated at room temperature with x rays, and then the spectrum was taken at 55 K with the magnetic field along the c direction. The microwave frequency was 9.406 GHz. Stick diagrams illustrate the separate hyperfine contributions from the ^{69}Ga and ^{71}Ga nuclei. (b) Simulated spectrum produced with the SimFonia computer program.

A related thermoluminescence (TL) peak is observed near 110 °C in our x-ray irradiated $LiGaO_2$ crystals. The emitted light associated with this TL peak has a maximum near 350 nm.

The S = 1/2 spectrum from the neutral lithium vacancies (V_{Li}^0) consists of a symmetrical pattern of resolved hyperfine lines with differing intensities caused by interactions with ^{69}Ga and ^{71}Ga nuclei. Both isotopes have I = 3/2 nuclear spins and they are 60.1% and 39.9% abundant, respectively. Their nuclear magnetic moments are $^{69}\mu = +2.0166\beta_n$ and $^{71}\mu = +2.5623\beta_n$.[24] The complicated V_{Li}^0 spectrum in Fig. 2(a) is explained by having nearly equal hyperfine interactions with Ga nuclei at two gallium sites adjacent to the trapped hole. This is consistent with our defect model since each oxygen ion in $LiGaO_2$ has two Li^+ ions and two Ga^{3+} ions as nearest neighbors. Thus, one Li^+ vacancy, one Li^+ ion, and two Ga^{3+} ions are adjacent to the trapped hole on the oxygen ion. Hyperfine lines from the ^{7}Li nucleus are not resolved in the V_{Li}^0 spectrum, whereas lines from the ^{69,71}Ga nuclei are well resolved. This agrees with our model, as atomic calculations[25,26] predict that the isotropic ^{7}Li hyperfine parameters will be approximately a factor of 30 smaller than the isotropic ^{69,71}Ga parameters when similar amounts of unpaired *s*-like spin density are on the Li and Ga ions.

With two adjacent sites for Ga, there are three combinations of the two Ga isotopes that contribute to the observed hyperfine pattern in Fig. 2(a). These are (i) two ^{69}Ga nuclei, (ii) one ^{69}Ga nucleus and one ^{71}Ga nucleus, and (iii) two ^{71}Ga nuclei. The relative distributions of these three combinations are 36.1%, 48.0%, and 15.9%, respectively. In Fig. 2(a), each combination is represented by a stick diagram above the experimental spectrum. Although the hyperfine interactions at the two Ga sites are not exactly equal, the stick diagrams are drawn for equal interactions. The relative lengths of the vertical lines in these diagrams reflect the natural abundances of the two Ga isotopes. The uppermost stick diagram illustrates the seven lines (with relative intensities of 1:2:3:4:3:2:1) that are produced when the unpaired spin interacts equally with two ^{69}Ga nuclei. The lowest stick diagram in Fig. 2(a) is the sum of the three upper stick diagrams and should be directly compared to the experimental spectrum. An EPR spectrum with a hyperfine pattern very similar to our V_{Li}^0 spectrum has been recently reported for the doubly ionized gallium vacancy (V_{Ga}^{2-}) in a β-Ga_2O_3 crystal.[27]

Evidence that the hyperfine interactions with the nuclei at the two neighboring Ga sites, although similar, are not equal is found in the relative intensities of the lines in the experimental spectrum in Fig. 2(a). If the two Ga sites have equal interactions, the intensity of the middle line in the spectrum should be a factor of 14.3 greater than the intensity of the lowest-field line. The experimental ratio in Fig. 2(a), however, is only about 8.5. This observed lower ratio suggests that the center line is slightly split due to inequivalent interactions at the neighboring Ga sites. This splitting is not resolved in the spectrum, but it does significantly reduce the intensity of the center line. The lowest-field line does not split when the two Ga sites have inequivalent interactions. Thus, unlike the center line, its intensity is unaffected by the inequivalency.

The experimental EPR spectrum in Fig. 2(a) has a set of underlying weak lines that slightly distort the V_{Li}^0 signals in the magnetic field region above 331.5 mT. Consequently, Ga hyperfine parameters that describe the *c* axis V_{Li}^0 spectrum were obtained from the undistorted low-field side. The lowest line and the middle line in Fig. 2(a) are separated by 9.675 mT. According to the ^{71}Ga-^{71}Ga stick diagram, the averaged value of $A_c(^{71}Ga)$ for these nuclei at the two Ga sites is equal to one-third of this separation. (Here, A_c represents the hyperfine interaction for each nucleus when the magnetic field is along the *c* direction.) This gives an averaged value of 3.22 mT for $A_c(^{71}Ga)$. A corresponding averaged value of 2.53 mT for $A_c(^{69}Ga)$ is obtained using the ratio of magnetic moments. A simulated *c* axis spectrum, produced with the SimFonia program from Bruker, is shown in Fig. 2(b). In this simulation, the hyperfine interactions at the two neighboring gallium sites are 4% different. The ^{69}Ga and ^{71}Ga parameters used in the simulation were 2.59 and 3.29 mT for one gallium site and 2.49 and 3.16 mT for the other gallium site.

Averaged hyperfine values for the ^{69,71}Ga nuclei at the two Ga sites adjacent to the trapped hole were also obtained for the V_{Li}^0 acceptor when the magnetic field was aligned along the *a* and *b* directions in the crystal. Results for the three directions (*a*, *b*, and *c*) are listed in Table II. For these high-symmetry directions, all crystallographically equivalent orientations of the defect are also magnetically equivalent, and the EPR spectra have their simplest form. Nearly identical hyperfine patterns were observed for each of the three directions of magnetic field, thus establishing the isotropic nature of the Ga interactions. The results in Table II provide direct evidence for the small-polaron model of the V_{Li}^0 acceptor. Specifically, small values for the strength of the Ga hyperfine interactions indicate that only 1.1% of the unpaired spin is in *4s* orbitals on the two Ga neighbors.[25] This leaves nearly all the remaining unpaired spin density in a *p* orbital on the oxygen ion.

The *g* values in Table II were obtained from measurements of the position of the center line in the V_{Li}^0 spectrum when the static magnetic field was along the *a*, *b*, and *c* directions. For these directions, the crystallographically equivalent orientations of the defect are all magnetically equivalent and the centers of the hyperfine patterns are easily identified. The EPR spectrum reached a minimum field

TABLE II. Parameters describing the EPR spectra of the neutral lithium vacancy (V_{Li}^0) in a $LiGaO_2$ crystal. The oxygen ion trapping the hole has two slightly inequivalent Ga neighbors. A *g* value and the average of the hyperfine parameters for the ^{69,71}Ga nuclei at the two sites were obtained when the magnetic field was along each of the three crystallographic axes. The estimated error is ±0.0005 for the *g* values and ±0.05 mT for the hyperfine values.

		Averaged hyperfine parameters (mT)	
Direction of magnetic field	*g* value	^{69}Ga	^{71}Ga
a crystal axis	2.0088	2.43	3.09
b crystal axis	2.0205	2.50	3.18
c crystal axis	2.0366	2.53	3.22

position (i.e., a turning point) when the magnetic field was along the *c* direction and reached a maximum field position when the magnetic field was near the *a* direction. These observations indicate that the principal axes of the *g* matrix are near the *a*, *b*, and *c* crystal directions and that the values listed in Table II are very near the principal values of the *g* matrix. The strong overlapping of lines caused by the presence of two magnetically inequivalent orientations of the defect prevented useful measurements of the angular dependence of the *g* matrix within the *a*-*b*, *b*-*c*, and *c*-*a* planes.

The small and positive *g* shifts observed for the V_{Li}^0 acceptor are consistent with a model that has the unpaired spin (i.e., the hole) located in a *p* orbital on one oxygen ion adjacent to the lithium vacancy. Acceptor-bound small polarons of this type have been extensively investigated in oxide crystals.[17,19,20,27] The oxygen trapping the hole is an O^- ion with a $2p^5$ configuration ($2p_x^2 2p_y^2 2p_z$). The local crystalline electric field removes the threefold orbital degeneracy of this ^2P state ($L = 1$, $S = 1/2$) and forms three energy levels (E_1, E_2, and E_3). In this simplified picture, E_1 is the ground state with the hole in the p_z orbital and E_2 and E_3 are excited states with the hole in the p_x and p_y orbitals of the ion, respectively. The spin-orbit interaction then mixes these excited states with the ground state and gives the following first-order expressions for the principal *g* values:[28]

$$g_1 = g_e, \quad g_2 = g_e - \frac{2\lambda}{E_2 - E_1}, \quad g_3 = g_e - \frac{2\lambda}{E_3 - E_1}. \quad (1)$$

The principal direction corresponding to the g_1 principal value is parallel to the unique axis of the p_z orbital. In these equations, the spin-orbit coupling constant λ for an O^- ion[29] is $-135\ cm^{-1}$ and g_e is 2.0023. The positive *g* shifts (i.e., values greater than 2.0023) reported in Table II for the V_{Li}^0 acceptor are a result of the negative sign for λ.

The value of 2.0088 for g_a in Table II is close to 2.0023, which suggests that the p_z orbital containing the unpaired spin is oriented near the *a* direction in the crystal. Figure 3 illustrates our proposed model for the V_{Li}^0 acceptor. The lithium vacancy is at the Li(1) position and the hole is localized on the adjacent $O_{II}(2)$ ion. Nuclei at the Ga(6) and Ga(7) sites are responsible for the resolved hyperfine structure seen in the EPR spectra. Before lattice relaxation, the Li(1) and $O_{II}(2)$ sites are 1.995 Å apart and the line joining them makes an angle of 18.2° with the *a* axis of the crystal. The p_z orbital representing the hole, shown in blue in Fig. 3, is pointing toward the center of the Li vacancy. This orientation of the p_z orbital corresponds to the minimum for the energy of the ground state of the neutral acceptor and establishes the importance of the electrostatic attraction between the positive hole and the "effective" negative charge of the lithium vacancy. The difference between the value of 2.0088 for g_a and an anticipated g_1 value nearer 2.0023 is explained by the relatively small 18.2° angle that the unique axis of the p_z orbital (and thus the principal direction for g_1) makes with the *a* direction in the crystal. In other words, the measured value of g_a is slightly greater than 2.0023 because the *a* direction, although close, is not a principal direction of the *g* matrix for the V_{Li}^0 acceptor.

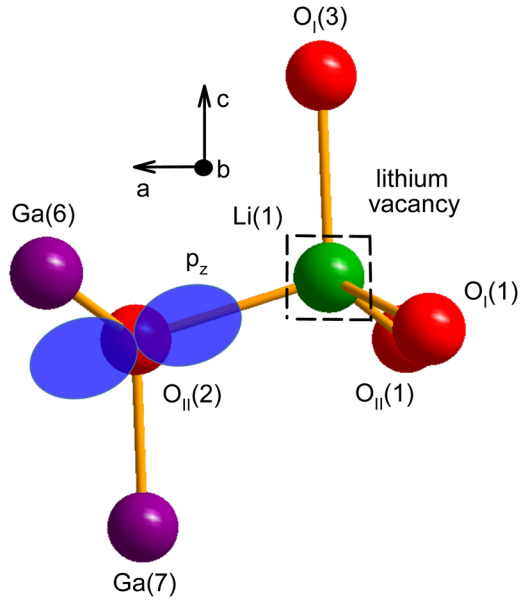

FIG. 3. Model of the neutral lithium vacancy (V_{Li}^0) in $LiGaO_2$. The trapped hole (shown in blue) is localized in a *p* orbital on the $O_{II}(2)$ oxygen ion with the lithium vacancy at the Li(1) position. The ^{69}Ga and ^{71}Ga nuclei at the Ga(6) and Ga(7) sites are responsible for the observed hyperfine.

IV. DOUBLY IONIZED GALLIUM VACANCY (V_{Ga}^{2-})

Figure 4(a) shows the EPR spectrum from the doubly ionized gallium vacancy (V_{Ga}^{2-}) in Sample B. This spectrum was taken at 93 K with the magnetic field along the *c* axis. There are six resolved hyperfine lines and g_c is 2.0032. These paramagnetic V_{Ga}^{2-} acceptors were produced by a "knock-on" process in the crystal during an irradiation near room temperature with 1 MeV electrons. A subsequent exposure to ionizing radiation was not needed, as the doubly ionized charge state of the gallium vacancy was thermally stable at room temperature in our crystal.

Similar to the V_{Li}^0 acceptor, the V_{Ga}^{2-} acceptor has a hole localized on one oxygen ion adjacent to the vacancy. With fewer hyperfine lines than the V_{Li}^0 spectrum, the experimental V_{Ga}^{2-} spectrum in Fig. 4(a) is explained by interactions with ^{69}Ga and ^{71}Ga nuclei at only one neighboring Ga site. This is consistent with our defect model since each oxygen ion in the $LiGaO_2$ crystal has two Li^+ ions and two Ga^{3+} ions as nearest neighbors. With one of the gallium ions missing, the oxygen ion with the trapped hole has two neighboring Li^+ ions and one neighboring Ga^{3+} ion. Hyperfine interactions with the adjacent ^7Li nuclei are not resolved in the V_{Ga}^{2-} spectrum, whereas interactions with the $^{69,71}Ga$ nuclei at the one neighboring Ga site are easily observed.

Each Ga isotope has an $I = 3/2$ nuclear spin and produces four equally spaced hyperfine lines, as illustrated by the stick diagrams above the experimental spectrum in Fig. 4(a). Only six lines are resolved in this spectrum because of the strong overlap of the middle lines within each set of four. The difference in the separation of hyperfine lines in the two sets is directly related to the ratio of the nuclear magnetic moments for ^{69}Ga and ^{71}Ga. From the line positions in Fig. 4(a), we find $A_c(^{69}Ga) = 3.59$ mT and

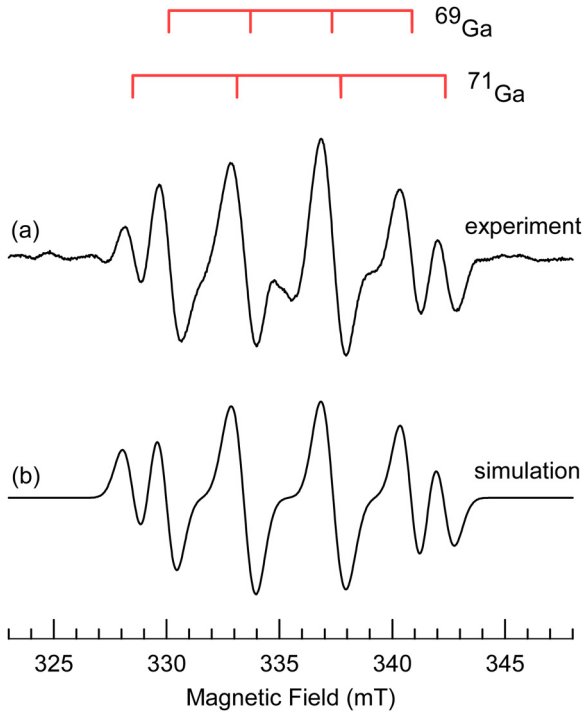

FIG. 4. (a) EPR spectrum of the doubly ionized gallium vacancy (V_{Ga}^{2-}) in $LiGaO_2$ (Sample B). The crystal was irradiated near room temperature with 1 MeV electrons. The spectrum was then taken at 93 K with the magnetic field along the *c* direction. The microwave frequency was 9.404 GHz. (b) A simulation spectrum produced with the SimFonia computer program.

$A_c(^{71}Ga) = 4.60$ mT for the V_{Ga}^{2-} acceptor. Using these results, the simulated *c*-axis spectrum shown in Fig. 4(b) was produced with the SimFonia program. Table III contains the experimental *g* values and hyperfine parameters for the V_{Ga}^{2-} acceptor when the magnetic field is along the *a*, *b*, and *c* directions. These results show that the ^{69}Ga and ^{71}Ga hyperfine matrices for the V_{Ga}^{2-} acceptor are nearly isotropic. The center of the EPR spectrum reached a minimum field position when the magnetic field was along the *b* direction and reached a maximum field position when the magnetic was near the *c* direction, thus indicating that the *g* values listed in Table III are very near the principal values of the *g* matrix.

The anisotropy of the *g* matrix is used to construct a model for the V_{Ga}^{2-} acceptor. When a hole is trapped on one oxygen ion next to a gallium vacancy, Eq. (1) predicts that one principal value of the *g* matrix will be very near 2.0023 and the other two principal values will have small, but positive, *g* shifts. The value of 2.0032 that we measure for g_c is very close to 2.0023, whereas the values for g_a and g_b are 2.0155 and 2.0551, respectively. This strongly suggests that the p_z orbital containing the unpaired electron spin is aligned along the *c* direction in the crystal. Our model for the V_{Ga}^{2-} acceptor in $LiGaO_2$ is shown in Fig. 5. The gallium vacancy is at the Ga(4) site and the hole is localized on the adjacent $O_{II}(4)$ ion. Nuclei at the Ga(3) site are responsible for the resolved hyperfine structure seen in the EPR spectra.

TABLE III. Parameters describing the EPR spectra of the doubly ionized gallium vacancy (V_{Ga}^{2-}) in a $LiGaO_2$ crystal. The oxygen ion trapping the hole has one Ga neighbor. A *g* value and the hyperfine parameters for the $^{69,71}Ga$ nuclei at the one site were obtained when the magnetic field was along each of the three crystallographic axes. The estimated error is ± 0.0005 for the *g* values and ±0.05 mT for the hyperfine values.

		Hyperfine parameters (mT)	
Direction of magnetic field	*g* value	^{69}Ga	^{71}Ga
a crystal axis	2.0155	3.75	4.76
b crystal axis	2.0551	3.74	4.75
c crystal axis	2.0032	3.59	4.60

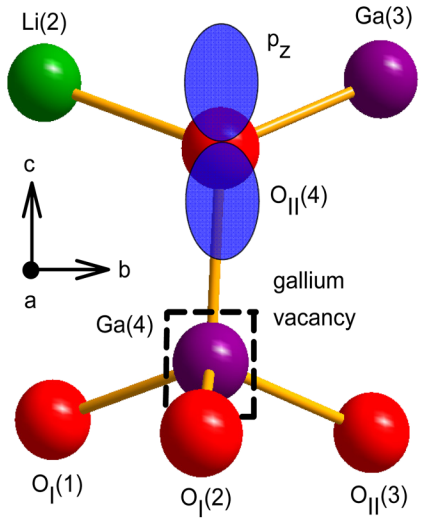

FIG. 5. Model of the doubly ionized gallium vacancy (V_{Ga}^{2-}) in $LiGaO_2$. The trapped hole (shown in blue) is localized in a *p* orbital on the $O_{II}(4)$ oxygen ion with the gallium vacancy at the Ga(4) position. The ^{69}Ga and ^{71}Ga nuclei at the Ga(3) site are responsible for the observed hyperfine.

V. SUMMARY

Electron paramagnetic resonance (EPR) has been used to identify and characterize native acceptors in wurtzite-like $LiGaO_2$ crystals. Neutral lithium vacancies (V_{Li}^0) and doubly ionized gallium vacancies (V_{Ga}^{2-}) are observed. These defects provide clear examples of acceptor-bound small polarons, where the unpaired spin (i.e., the hole) is localized on one oxygen ion adjacent to the vacancy. Resolved hyperfine structure from neighboring $^{69,71}Ga$ nuclei and anisotropy in the *g* matrices are used to construct specific models for these acceptors. In both defects, the hole is located at an O_{II} ion, as it forms the shortest bond with neighboring lithium and gallium ions.

The thermal stability of the paramagnetic charge states of these cation vacancies at room temperature is days for V_{Li}^0 and more than one year for V_{Ga}^{2-}. This suggests that they are deep levels, as expected for acceptor-bound polarons in oxide crystals. If acceptors such as Mg can be placed on a Ga site in Li-rich, Ga-poor material, their neutral state may also be deep, and thus not useful for devices, because of the formation of similar small polarons. In the search for suitable *p*-type dopants for $LiGaO_2$, nitrogen ions replacing oxygen ions may be a more likely solution.

ACKNOWLEDGMENTS

Work at the Air Force Institute of Technology (AFIT) was supported by the Air Force Office of Scientific Research (AFOSR) under Award No. F4FGA08054J003.

The views expressed in this paper are those of the authors and do not necessarily reflect the official policy or position of the Air Force, the Department of Defense, or the United States Government.

[1]I. Suzuki and T. Omata, "Multinary wurtzite-type oxide semiconductors: Present status and perspectives," Semicond. Sci. Technol. **32**, 013007 (2017).
[2]T. Omata, H. Nagatani, I. Suzuki, and M. Kita, "Wurtzite-derived ternary I-III-O_2 semiconductors," Sci. Technol. Adv. Mater. **16**, 024902 (2015).
[3]C. Chen, C. Li, S. Yu, and M. M. C. Chou, "Growth and characterization of β-$LiGaO_2$ single crystal," J. Cryst. Growth **402**, 325 (2014).
[4]S. Tumėnas, P. Mackonis, R. Nedzinskas, L. Trinkler, B. Berzina, V. Korsaks, L. Chang, and M. M. C. Chou, "Optical properties of lithium gallium oxide," Appl. Surf. Sci. **421**, 837 (2017).
[5]N. W. Johnson, J. A. McLeod, and A. Moewes, "The electronic structure of lithium metagallate," J. Phys.: Condens. Matter **23**, 445501 (2011).
[6]A. Boonchun and W. R. L. Lambrecht, "First-principles study of the elasticity, piezoelectricity, and vibrational modes in $LiGaO_2$ compared with ZnO and GaN," Phys. Rev. B **81**, 235214 (2010). See also Phys. Rev. B **82**, 079904 (2010).
[7]S. N. Rashkeev, S. Limpijumnong, and W. R. L. Lambrecht, "Theoretical evaluation of $LiGaO_2$ for frequency upconversion to ultraviolet," J. Opt. Soc. Am. B **16**, 2217 (1999).
[8]T. Omata, M. Kita, K. Tachibana, and S. Otsuka-Yao-Matsuo, "Structural variation and optical properties of ZnO-LiGaO2 pseudo-binary system," J. Solid State Chem. **188**, 92 (2012).
[9]Q. F. Li and J. Kuo, "First-principles study of band gap engineering of ZnO by alloying with $LiGaO_2$ for ultraviolet applications," J. Appl. Phys. **114**, 063715 (2013).
[10]T. Omata, K. Tanaka, A. Tazuke, K. Nose, and S. Otsuka-Yao-Matsuo, "Wide band gap semiconductor alloy: $x(LiGaO_2)_{1/2}$-(1-x)ZnO," J. Appl. Phys. **103**, 083706 (2008).
[11]A. Boonchun and W. R. L. Lambrecht, "Electronic structure, doping and lattice dynamics of $LiGaO_2$," Proc. SPIE **7940**, 79400N (2011).
[12]M. S. Holston, I. P. Ferguson, N. C. Giles, J. W. McClory, D. J. Winarski, J. Ji, F. A. Selim, and L. E. Halliburton, "Green luminescence from Cu-diffused $LiGaO_2$ crystals," J. Lumin. **170**, 17 (2016).
[13]T. Yanagida, Y. Fujimoto, M. Koshimizu, N. Kawano, G. Okada, and N. Kawaguchi, "Comparative studies of optical and scintillation properties between $LiGaO_2$ and $LiAlO_2$ crystals," J. Phys. Soc. Jpn. **86**, 094201 (2017).
[14]L. Trinkler, A. Trukhin, B. Berzina, V. Korsaks, P. Ŝĉajev, R. Nedzinskas, S. Tumėnas, M. M. C. Chou, L. Chang, and C.-A. Li, "Luminescence properties of $LiGaO_2$ crystal," Opt. Mater. **69**, 449 (2017).
[15]S. Kück and S. Hartung, "Comparative study of the spectroscopic properties of Cr^{4+}-doped $LiAlO_2$ and $LiGaO_2$," Chem. Phys. **240**, 387 (1999).
[16]G. J. Dirksen, A. N. J. M. Hoffman, T. P. Vandebout, M. P. G. Laudy, and G. Blasse, "Luminescence spectra of pure and doped $GaBO_3$ and $LiGaO_2$," J. Mater. Chem. **1**, 1001 (1991).
[17]M. S. Holston, J. W. McClory, N. C. Giles, and L. E. Halliburton, "Radiation-induced defects in $LiAlO_2$ crystals: Holes trapped by lithium vacancies and their role in thermoluminescence," J. Lumin. **160**, 43 (2015).
[18]M. S. Holston, I. P. Ferguson, J. W. McClory, N. C. Giles, and L. E. Halliburton, "Oxygen vacancies in $LiAlO_2$ crystals," Phys. Rev. B **92**, 144108 (2015).
[19]A. M. Stoneham, J. Gavartin, A. L. Shluger, A. V. Kimmel, D. M. Ramo, H. M. Rønnow, G. Aeppli, and C. Renner, "Trapping, self-trapping and the polaron family," J. Phys.: Condens. Matter **19**, 255208 (2007).
[20]O. F. Schirmer, "O^- bound small polarons in oxide materials," J. Phys.: Condens. Matter **18**, R667 (2006).
[21]M. M. Islam, J. Uhlendorf, E. Witt, H. Schmidt, P. Heitjans, and T. Bredow, "Lithium diffusion mechanisms in β-$LiMO_2$ (M = Al, Ga): A combined experimental and theoretical study," J. Phys. Chem. C **121**, 27788 (2017).
[22]C. V. Chandran, K. Volgmann, S. Nakhal, R. Uecker, E. Witt, M. Lerch, and P. Heitjans, "Local ion dynamics in polycrystalline β-$LiGaO_2$: A solid-state NMR study," Z. Phys. Chem. **231**, 1443 (2017).
[23]M. Marezio, "Crystal structure of $LiGaO_2$," Acta Crystallogr. **18**, 481 (1965).
[24]N. J. Stone, "Table of nuclear magnetic dipole and electric quadrupole moments," At. Data Nucl. Data Tables **90**, 75 (2005).
[25]J. R. Morton and K. F. Preston, "Atomic parameters for paramagnetic resonance data," J. Magn. Reson. **30**, 577 (1978).
[26]J. A. J. Fitzpatrick, F. R. Manby, and C. M. Western, "The interpretation of molecular magnetic hyperfine interactions," J. Chem. Phys. **122**, 084312 (2005).
[27]B. E. Kananen, L. E. Halliburton, K. T. Stevens, G. K. Foundos, and N. C. Giles, "Gallium vacancies in β-Ga_2O_3 crystals," Appl. Phys. Lett. **110**, 202104 (2017).
[28]J. A. Weil and J. R. Bolton, *Electron Paramagnetic Resonance: Elementary Theory and Practical Applications*, 2nd ed. (John Wiley and Sons, Hoboken, NJ, 2007), Chap. 4, pp. 108–109.
[29]R. H. Bartram, C. E. Swenberg, and J. T. Fournier, "Theory of trapped-hole centers in aluminum oxide," Phys. Rev. **139**, A941 (1965).